Investigations on the light hadron decays of $Z_b(10610)$ and $Z_b(10650)$

Qi Wu,[1,*] Yuanxin Zheng,[2,†] Shidong Liu,[2,‡] and Gang Li[2,§]

[1]School of Physics and Center of High Energy Physics, Peking University, Beijing 100871, China
[2]School of Physics and Physical Engineering, Qufu Normal University, Qufu 273165, China

(Received 8 November 2022; accepted 10 February 2023; published 24 February 2023)

The light hadron decay processes of $Z_b(10610)/Z_b(10650)$ provide us a way to study their nature and decay mechanism. In this work, we evaluate the branching ratios of $Z_b(10610)/Z_b(10650) \to VP$ (V and P stand for light vector and pseudoscalar mesons, respectively) using an effective Lagrangian approach, in which the contributions of intermediate bottomed meson triangle loops are considered. In our calculations, the $Z_b(10610)$ and $Z_b(10650)$ are regarded as $B\bar{B}^* + \text{c.c.}$ and $B^*\bar{B}^*$ molecular states, respectively. The predicted branching ratios of $Z_b(10610) \to VP$ are about in the order of 10^{-2}, while the branching ratios of $Z_b(10650) \to VP$ are in the order of 10^{-3}. Furthermore, the dependence of these ratios between different decay modes of $Z_b(10610)/Z_b(10650)$ on the mixing $\eta - \eta'$ angle θ_P is investigated, which may be a good quantity for the experiments. It is hoped that the calculations here could be tested by future experiments.

DOI: 10.1103/PhysRevD.107.034028

I. INTRODUCTION

The discovery of $X(3872)$ in 2003 opens the gate to the XYZ states in the heavy quarkonium region [1]. A large number of experimental and theoretical studies have been devoted to the XYZ states (see Refs. [2–14] for recent reviews). Many of them cannot be accommodated in the conventional quark model as $Q\bar{Q}$ and thus turn out to be excellent candidates for exotic states.

In the charm sector, many charmoniumlike states, such as $Z_c(3900)/Z_c(4020)/Z_{cs}(3985)$ [15,16], $T_{cc}^+(3875)$ [17,18], $X(6900)$ [19], and P_c/P_{cs} [20–24], have been observed experimentally. However, in the bottom sector, only two bottomoniumlike states $Z_b(10610)$ and $Z_b(10650)$, hereafter referred to as $Z_b^{\pm,0}$ and $Z_b'^{\pm,0}$, respectively, were observed in the invariant mass distributions of the $\pi^\pm\Upsilon(nS)$ ($n = 1, 2, 3$) and $\pi^\pm h_b(mP)$ ($m = 1, 2$) final states in the processes $\Upsilon(5S) \to \pi^\pm\pi^\mp\Upsilon(nS)$ and $\Upsilon(5S) \to \pi^\pm\pi^\mp h_b(mP)$ [25] by the Belle Collaboration in 2011. The charged pion angular distribution analysis [26] indicates that the quantum number of the two states favors $I^G(J^P) = 1^+(1^+)$. Furthermore, the amplitude analysis of $e^+e^- \to \Upsilon(nS)\pi^+\pi^-$ [27] confirms $I^G(J^P) = 1^+(1^+)$ for Z_b and Z_b'. The neutral state Z_b^0 was observed in a Dalitz analysis of $\Upsilon(5S) \to \pi^0\pi^0\Upsilon(nS)$ decays by the Belle Collaboration [28,29], which indicates that $Z_b^{(\prime)}$ are isovector states. Therefore, they contain at least four constituent quarks and thus are ideal candidates of the exotic hadronic state.

The peculiar natures of $Z_b^{(\prime)}$ intrigued theorists to explore their inner structure. Since the masses of Z_b and Z_b' are very close to the thresholds of $B\bar{B}^* + \text{c.c.}$ and $B^*\bar{B}^*$, respectively, they are naturally regarded as the deuteronlike molecular states composed of $B\bar{B}^* + \text{c.c.}$ and $B^*\bar{B}^*$ [30–49], which could explain most of the properties of $Z_b^{(\prime)}$. The authors in Ref. [30] pointed out that the observations with similar rates of the $Z_b^{(\prime)}$ in both the final states containing the spin-triplet $\Upsilon(1S, 2S, 3S)$ and spin-singlet $h_b(1P, 2P)$ can be naturally understood since the $b\bar{b}$ pairs in both Z_b and Z_b' are mixtures of a spin-triplet and a spin-singlet in the molecular states scenario. In the framework of the one-boson-exchange model, Z_b and Z_b' can be interpreted as the $B\bar{B}^*$ and $B^*\bar{B}^*$ molecular states [31]. In the molecular states picture, the masses of $Z_b^{(\prime)}$ could be well reproduced using QCD sum rules [37–39]. Besides, many studies of the decays [40–47] and productions [48,49] of $Z_b^{(\prime)}$ also support the molecule interpretation. It seems that $Z_b^{(\prime)}$ are molecular states composed of $B\bar{B}^* + \text{c.c.}$ and $B^*\bar{B}^*$, but other interpretations could not be ruled out. For example, it is interpreted as the tetraquark states with four valence quarks ($b\bar{b}q\bar{q}, q = u, d$) since $Z_b^{(\prime)}$ were observed in the $\pi\Upsilon(1S, 2S, 3S)$ and $\pi h_b(1P, 2P)$ invariant mass spectrum. With the help of

*wu_qi@pku.edu.cn
†13563834773@163.com
‡Corresponding author.
liusd@qfnu.edu.cn
§Corresponding author.
gli@qfnu.edu.cn

TABLE I. Measurements of the branching ratios (%) of Z_b and Z_b' from PDG [58].

Decay channels	Z_b^+	$Z_b'^+$
$\Upsilon(1S)\pi^+$	$0.54^{+0.19}_{-0.15}$	$0.17^{+0.08}_{-0.06}$
$\Upsilon(2S)\pi^+$	$3.6^{+1.1}_{-0.8}$	$1.4^{+0.6}_{-0.4}$
$\Upsilon(3S)\pi^+$	$2.1^{+0.8}_{-0.6}$	$1.6^{+0.7}_{-0.5}$
$h_b(1P)\pi^+$	$3.5^{+1.2}_{-0.9}$	$8.4^{+2.9}_{-2.4}$
$h_b(2P)\pi^+$	$4.7^{+1.7}_{-1.3}$	15 ± 4
$B^+\bar{B}^{*0} + B^{*+}\bar{B}^0$	$85.6^{+2.1}_{-2.9}$	...
$B^{*+}\bar{B}^{*0}$	...	74^{+4}_{-6}

various models, different possible tetraquark state configurations of $Z_b^{(\prime)}$ were investigated [50–52]. Besides the QCD exotic interpretations, the structures corresponding to $Z_b^{(\prime)}$ could be reproduced through initial-single-pion-emission mechanism [53,54] or cusp effect [55,56].

In addition to the mass spectrum studies, the decays and productions also contain detailed dynamical information and hence provide another perspective about their properties. The productions of $Z_b^{(\prime)}$ states from the $\Upsilon(5S)$ radiative decays and hidden bottom decays were studied with Z_b and Z_b' being $B\bar{B}^* + \text{c.c.}$ and $B^*\bar{B}^*$ hadronic molecules, respectively [48,49]. The hidden-bottom and radiative decays of $Z_b^{(\prime)}$ have been extensively investigated using various methods. $Z_b^{(\prime)} \to \Upsilon(nS)\pi$ was evaluated in a phenomenological Lagrangian approach in Ref. [40]. QCD multipole expansion was applied to study the ratios of the decay rates of $Z_b^{(\prime)} \to \Upsilon(nS)\pi$ and $Z_b^{(\prime)} \to h_b(mP)\pi$ in Ref. [44]. By adopting an effective Lagrangian approach, the authors in Refs. [41,42,46] evaluated the bottom meson loop contributions of $Z_b^{(\prime)} \to \Upsilon(nS)\pi$, $Z_b^{(\prime)} \to h_b(mP)\pi$, and $Z_b^{(\prime)} \to \eta_b(mP)\gamma$. The decays $Z_b^{(\prime)} \to \Upsilon(nS)\pi$, $Z_b^{(\prime)} \to h_b(mP)\pi$, and $Z_b^{(\prime)} \to \chi_{bJ}(mP)\gamma$ were investigated within a nonrelativistic effective field theory in Ref. [43].

Besides the resonance parameters of the $Z_b^{(\prime)}$ states, the Belle Collaboration also measured the open-bottom and hidden-bottom decay modes of $Z_b^{\pm}$ and $Z_b^{\pm}$ in $\Upsilon(5S)$ decays [57]. In Table I, we list the branching ratios of Z_b^+ and $Z_b'^+$ obtained from Particle Data Group (PDG) [58]. It can be seen that the dominant decay modes of $Z_b^+/Z_b'^+$ are open-bottom decays, i.e., Z_b^+ and $Z_b'^+$ mainly decay into $B^+\bar{B}^{*0} + \text{c.c.}$ with branching ratio $(85.6^{+2.1}_{-2.9})\%$ and $B^{*+}\bar{B}^{*0}$ with branching ratio $74^{+4}_{-6}\%$, respectively. The secondary decay modes of Z_b^+ and $Z_b'^+$ are the hidden-bottom decay, namely $\pi^+\Upsilon(nS)$ $(n = 1, 2, 3)$ and $\pi^+ h_b(mP)$ $(m = 1, 2)$. The branching ratios are $14.4^{+2.5}_{-1.9}\%$ for $Z_b^+ \to (b\bar{b}) + \pi^+$ and $26.6^{+5.0}_{-4.7}\%$ for $Z_b'^+ \to (b\bar{b}) + \pi^+$. To better understand the nature of $Z_b^{(\prime)}$, the study of other decay modes is necessary. For example, the light hadron decay modes can provide a good platform to study their nature. In Refs. [59,60], we have investigated the charmless decays of charmoniunlike states $Z_c(3900)/Z_c(4020)$ and $X(3872)$ by considering the contributions of intermediate charmed meson loops, and predicted accessible decay rates. In this work, we investigate the light hadron decay modes of $Z_b^{(\prime)} \to VP$ via the intermediate bottomed meson loops using an effective Lagrangian approach. We will focus on the light hadron decays of Z_b^+ and $Z_b'^+$. For simplicity, we do not distinguish the charged and the neutral $Z_b^{(\prime)}$ states and use $Z_b^{(\prime)}$ to represent $Z_b^{(\prime)+}$.

This article is organized as follows. After the Introduction, we present the theoretical framework used in Sec. II. The numerical results and discussion are presented in Sec. III, and a brief summary is given in Sec. IV.

II. THEORETICAL FRAMEWORK

We study the light hadron decays of $Z_b^{(\prime)}$ states using the effective Lagrangian approach. The experimental measurements reveal that Z_b and Z_b' dominantly decay into $B\bar{B}^* + \text{c.c.}$ and $B^*\bar{B}^*$, leading to strong couplings of Z_b and Z_b' to $B\bar{B}^* + \text{c.c.}$ and $B^*\bar{B}^*$. Their light hadron decays can be proceeded by the triangle diagrams as shown in Figs. 1 and 2, each of which has three bottomed mesons in the triangle loop. In the following, we apply such a mechanism to study the light hadron decays of Z_b and Z_b'.

A. Effective Lagrangian

To calculate the triangle loops shown in Figs. 1 and 2, we need the effective couplings of the Z_b and Z_b' states to $B\bar{B}^*$ and $B^*\bar{B}^*$ channels, respectively. The effective Lagrangians describing the couplings of Z_b and Z_b' states to $B\bar{B}^*$ and $B^*\bar{B}^*$ channels via S wave are written as [43]

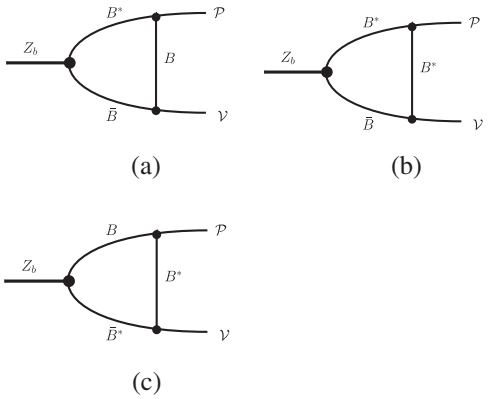

FIG. 1. The hadron-level diagrams contributing to the light hadron decays $Z_b \to VP$. The charge conjugated diagrams are not shown but included in our calculations.

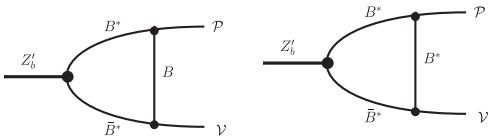

(a) (b)

FIG. 2. The hadron-level diagrams contributing to the light hadron decays $Z_b' \to VP$. The charge conjugated diagrams are not shown but included in our calculations.

$$\mathcal{L}_{Z_b^{(\prime)}B^{(*)}B^{(*)}} = g_{Z_bBB^*} Z_b^{\mu}(BB_{\mu}^{*\dagger} + B_{\mu}^{*}B^{\dagger}) + g_{Z_b'B^*B^*}\epsilon_{\mu\nu\alpha\beta}\partial^{\mu}Z_b'^{\nu}B^{*\alpha}B^{*\dagger\beta} + \text{H.c.}, \quad (1)$$

where $B^{(*)} = (B^{(*)+}, B^{(*)0}, B_s^{(*)0})$ is the bottom meson triplets; $g_{Z_bBB^*}$ and $g_{Z_b'B^*B^*}$ are the coupling constants. We use the convention $\varepsilon_{0123} = +1$. Here we should notice that the Lagrangians in Ref. [43] are the nonrelativistic form of Eq. (1). In the nonrelativistic limit, the Lagrangians in Eq. (1) can back to the form in Ref. [43]. With the above effective Lagrangians, we can obtain

$$\Gamma_{Z_b\to B^+\bar{B}^{*0}+B^{*+}\bar{B}^0} = \frac{|\vec{q}_B|}{12\pi m_{Z_b}^2} g_{Z_bBB^*}^2 \left(\frac{|\vec{q}_B|^2}{m_{B^*}^2} + 3\right), \quad (2)$$

$$\Gamma_{Z_b'\to B^{*+}\bar{B}^{*0}} = \frac{|\vec{q}_{B^*}|}{24\pi} g_{Z_b'B^*B^*}^2 \left(\frac{m_{Z_b'}^2}{m_{B^*}^2} + 2\right), \quad (3)$$

with $\vec{q}_B$ and $\vec{q}_{B^*}$ being the three-momenta of the B and B^* mesons in the rest frame of Z_b and Z_b', respectively. With the experimentally measured branching ratios $\text{BR}(Z_b \to B^+\bar{B}^{*0} + B^{*+}\bar{B}^0) = 85.6\%$, $\text{BR}(Z_b' \to B^{*+}\bar{B}^{*0}) = 74\%$ shown in Table I, and the center values of the total widths of $Z_b^{(\prime)}$, we can get the relevant couplings $g_{Z_bBB^*} = 13.23$ GeV and $g_{Z_b'B^*B^*} = 0.94$, respectively. The coupling constants between ours and Ref. [43] are consistent, and they have the following relationship:

$$g_{Z_bBB^*} = z\sqrt{m_{Z_b} m_B m_{B^*}}, \qquad g_{Z_b'B^*B^*} = z' \frac{m_{B^*}}{\sqrt{m_{Z_b'}}}, \quad (4)$$

where $z = 0.77\ \text{GeV}^{-1/2}$ and $z' = 0.57\ \text{GeV}^{-1/2}$. Note that $g_{Z_b^{(\prime)}B^{(*)}B^*}$ and $z^{(\prime)}$ differ in some mass factors. As indicated in Ref. [43], for very-near-threshold states, small differences in masses may imply huge differences in binding energies resulting in significantly different effective couplings. Thus, a small difference between the couplings z and z' is reasonable.

Here we should also notice that the $Z_b(10610)$ and $Z_b(10650)$ are very close to the thresholds of $B\bar{B}^*$ and $B^*\bar{B}^*$, so the threshold effects may be a possible explanation. Authors in [55,56] pointed that the threshold cusps at $B\bar{B}^*$ and $B^*\bar{B}^*$ thresholds are capable of explaining the peaks observed by Belle. If these states are threshold effects, no coupling of a state to $B\bar{B}^*$ or $B^*\bar{B}^*$ can be defined. To date, none of the explanations have been ruled out. Indeed, the nature of the $Z_b^{(\prime)}$ states lie closely to $B^{(*)}\bar{B}^{(*)}$ threshold not only arises the molecular state composed of $B^{(*)}\bar{B}^{(*)}$ but also the threshold effects. As demonstrated in [61], these two narrow peaks cannot be purely kinematic effects.

The present work is based on the fact that Z_b and Z_b' dominant decay to $B\bar{B}^*$ and $B^*\bar{B}^*$ and the branching ratios of $Z_b \to B\bar{B}^*$ and $Z_b' \to B^*\bar{B}^*$ have been measured by experiments. With these experimental measurements and effective interactions, we extract the coupling constants $g_{Z_bB\bar{B}^*}$ and $g_{Z_b'B^*\bar{B}^*}$. Since we start from the assumption that the $Z_b^{(\prime)}$ states have strong couplings to $B\bar{B}^*$ and $B^*\bar{B}^*$, their decays into the light hadron states can happen only via the B meson loops. As the $Z_b^{(\prime)}$ decay to $B^{(*)}\bar{B}^*$ is on-shell and thus real processes, the intermediate states $B^{(*)}\bar{B}^*$ can be cut off. Such a rescattering process can be understood by Cutkosky rule [62]: $Z_b^{(\prime)}$ first decay to $B^{(*)}\bar{B}^*$, $B^{(*)}$ and $\bar{B}^*$ rescattering to the light hadron final states through exchanging a proper B meson. In this scenario, the branching ratios of $Z_b^{(\prime)} \to B^{(*)}\bar{B}^*$ are consistent with the experimental data as long as we take the coupling constants extracted from the experiment as input. Thus, the couplings of $Z_b^{(\prime)}$ do not cause large uncertainties.

On the other hand, the Lagrangians relevant to the light vector and pseudoscalar mesons can be constructed based on the heavy quark limit and chiral symmetry [63–65]

$$\begin{aligned}\mathcal{L} =& -ig_{B^*B\mathcal{P}}(B_i^{\dagger}\partial_{\mu}\mathcal{P}_{ij}B_j^{*\mu} - B_i^{*\mu\dagger}\partial_{\mu}\mathcal{P}_{ij}B_j) \\ &+ \frac{1}{2}g_{B^*B^*\mathcal{P}}\varepsilon_{\mu\nu\alpha\beta}B_i^{*\mu\dagger}\partial^{\nu}\mathcal{P}_{ij}\overleftrightarrow{\partial}^{\alpha}B_j^{*\beta} - ig_{BB\mathcal{V}}B_i^{\dagger}\overleftrightarrow{\partial}_{\mu}B^j(\mathcal{V}^{\mu})_j^i \\ &- 2f_{B^*B\mathcal{V}}\epsilon_{\mu\nu\alpha\beta}(\partial^{\mu}\mathcal{V}^{\nu})_j^i(B_i^{\dagger}\overleftrightarrow{\partial}^{\alpha}B^{*\beta j} - B_i^{*\beta\dagger}\overleftrightarrow{\partial}^{\alpha}B^j) \\ &+ ig_{B^*B^*\mathcal{V}}B_i^{*\nu\dagger}\overleftrightarrow{\partial}_{\mu}B_{\nu}^{*j}(\mathcal{V}^{\mu})_j^i \\ &+ 4if_{B^*B^*\mathcal{V}}B_{i\mu}^{*\dagger}(\partial^{\mu}\mathcal{V}^{\nu} - \partial^{\nu}\mathcal{V}^{\mu})_j^i B_{\nu}^{*j} + \text{H.c.} \end{aligned} \quad (5)$$

Again, $B^{(*)} = (B^{(*)+}, B^{(*)0}, B_s^{(*)0})$ is the bottom meson triplets; $\mathcal{P}$ and $\mathcal{V}_{\mu}$ are 3×3 matrices representing the pseudoscalar and vector mesons, and their specific forms are

$$\mathcal{P} = \begin{pmatrix} \frac{\pi^0}{\sqrt{2}} + \frac{\beta\eta+\gamma\eta'}{\sqrt{2}} & \pi^+ & K^+ \\ \pi^- & -\frac{\pi^0}{\sqrt{2}} + \frac{\beta\eta+\gamma\eta'}{\sqrt{2}} & K^0 \\ K^- & \bar{K}^0 & -\gamma\eta + \beta\eta' \end{pmatrix},$$

$$\mathcal{V} = \begin{pmatrix} \frac{\rho^0}{\sqrt{2}} + \frac{\omega}{\sqrt{2}} & \rho^+ & K^{*+} \\ \rho^- & -\frac{\rho^0}{\sqrt{2}} + \frac{\omega}{\sqrt{2}} & K^{*0} \\ K^{*-} & \bar{K}^{*0} & \phi \end{pmatrix}. \quad (6)$$

The physical states η and η' are the mixing of favor eigenstates $n\bar{n} = (u\bar{u} + d\bar{d})/\sqrt{2}$ and $s\bar{s}$, which have the following wave functions:

$$|\eta\rangle = \beta|n\bar{n}\rangle - \gamma|s\bar{s}\rangle,$$
$$|\eta'\rangle = \gamma|n\bar{n}\rangle + \beta|s\bar{s}\rangle, \tag{7}$$

where $\beta = \cos\alpha_P$, $\gamma = \sin\alpha_P$, with $\alpha_P \simeq \theta_P + \arctan\sqrt{2}$. The empirical value for the pseudoscalar mixing angle θ_P is in the range $[-24.6°, -11.5°]$ [58].

In the heavy quark and chiral limits, the couplings of bottomed mesons to the light vector mesons have the following relationships [63,65]:

$$g_{BBV} = g_{B^*B^*V} = \frac{\beta g_V}{\sqrt{2}}, \qquad f_{B^*BV} = \frac{f_{B^*B^*V}}{m_{B^*}} = \frac{\lambda g_V}{\sqrt{2}},$$
$$g_{B^*B\mathcal{P}} = \frac{2g}{f_\pi}\sqrt{m_B m_{B^*}}, \qquad g_{B^*B^*P} = \frac{g_{B^*B\mathcal{P}}}{\sqrt{m_B m_{B^*}}}. \tag{8}$$

In this work, we take the parameters $\beta = 0.9$, $\lambda = 0.56\ \mathrm{GeV}^{-1}$, $g = 0.59$, and $g_V = m_\rho/f_\pi$ with $f_\pi = 132$ MeV as used in previous works [63,66]. The uncertainties resulting from SU(3) breaking effects have been embodied in the relations given in Eq. (8).

B. Decay amplitude

With the above effective Lagrangians, the decay amplitudes of these triangle diagrams in Figs. 1 and 2 can easily be obtained. For $Z_b(p_1) \to [B^{(*)}(q_1)\bar{B}^{(*)}(q_3)]B^{(*)}(q_2) \to V(p_2)P(p_3)$ shown in Fig. 1, the explicit amplitudes are

$$\mathcal{M}_a^{Z_b} = i^3 \int \frac{d^4q}{(2\pi)^4}[g_{Z_bBB^*}\epsilon_{1\mu}][g_{B^*BP}p_{3\nu}][g_{BBV}\epsilon^*_{2\alpha}(q_3^\alpha - q_2^\alpha)]\frac{-g^{\mu\nu} + q_1^\mu q_1^\nu/m_1^2}{q_1^2 - m_1^2}\frac{1}{q_2^2 - m_2^2}\frac{1}{q_3^2 - m_3^2}\prod_i \mathcal{F}_i(q_i^2),$$
$$\mathcal{M}_b^{Z_b} = i^3 \int \frac{d^4q}{(2\pi)^4}[g_{Z_bBB^*}\epsilon_{1\kappa}]\left[\frac{1}{2}g_{B^*B^*P}\varepsilon_{\mu\nu\alpha\beta}p_3^\nu(q_1^\alpha + q_2^\alpha)\right][-2f_{B^*BV}\varepsilon_{\rho\sigma\tau\xi}p_2^\rho\epsilon_2^{*\sigma}(q_2^\tau - q_3^\tau)]$$
$$\times\frac{-g^{\kappa\beta} + q_1^\kappa q_1^\beta/m_1^2}{q_1^2 - m_1^2}\frac{-g^{\mu\xi} + q_2^\mu q_2^\xi/m_2^2}{q_2^2 - m_2^2}\frac{1}{q_3^2 - m_3^2}\prod_i \mathcal{F}_i(q_i^2),$$
$$\mathcal{M}_c^{Z_b} = i^3 \int \frac{d^4q}{(2\pi)^4}[g_{Z_bBB^*}\epsilon_{1\rho}][-g_{B^*BP}p_{3\sigma}][g_{B^*B^*V}g_{\tau\theta}(q_{2\kappa} - q_{3\kappa})\epsilon_2^{*\kappa} + 4if_{B^*B^*V}(-p_{2\tau}\epsilon^*_{2\theta} + p_{2\theta}\epsilon^*_{2\tau})]$$
$$\times\frac{1}{q_1^2 - m_1^2}\frac{-g^{\sigma\theta} + q_2^\sigma q_2^\theta/m_2^2}{q_2^2 - m_2^2}\frac{-g^{\rho\tau} + q_3^\rho q_3^\tau/m_3^2}{q_3^2 - m_3^2}\prod_i \mathcal{F}_i(q_i^2). \tag{9}$$

The explicit transition amplitudes for $Z_b'(p_1) \to [B^*(q_1)\bar{B}^*(q_3)]B^{(*)}(q_2) \to V(p_2)P(p_3)$ in Fig. 2 are

$$\mathcal{M}_a^{Z_b'} = i^3 \int \frac{d^4q}{(2\pi)^4}[ig_{Z_b'B^*B^*}\varepsilon_{\mu\nu\alpha\beta}p_1^\mu\epsilon_1^\nu][g_{B^*BP}p_{3\lambda}][2f_{B^*BV}\varepsilon_{\rho\sigma\tau\xi}p_2^\rho\epsilon_2^{*\sigma}(q_2^\tau - q_3^\tau)]$$
$$\times\frac{-g^{\alpha\lambda} + q_1^\alpha q_1^\lambda/m_1^2}{q_1^2 - m_1^2}\frac{1}{q_2^2 - m_2^2}\frac{-g^{\beta\xi} + q_3^\beta q_3^\xi/m_3^2}{q_3^2 - m_3^2}\prod_i \mathcal{F}_i(q_i^2),$$
$$\mathcal{M}_b^{Z_b'} = i^3 \int \frac{d^4q}{(2\pi)^4}[ig_{Z_b'B^*B^*}\varepsilon_{\mu\nu\alpha\beta}p_1^\mu\epsilon_1^\nu]\left[\frac{1}{2}g_{B^*B^*P}\varepsilon_{\rho\sigma\lambda\xi}p_3^\sigma(q_1^\lambda + q_2^\lambda)\right][g_{B^*B^*V}g_{\tau\theta}(q_{2\kappa} - q_{3\kappa})\epsilon_2^{*\kappa} + 4f_{B^*B^*V}(p_{2\theta}\epsilon^*_{2\tau} - p_{2\tau}\epsilon^*_{2\theta})]$$
$$\times\frac{-g^{\alpha\xi} + q_1^\alpha q_1^\xi/m_1^2}{q_1^2 - m_1^2}\frac{-g^{\rho\theta} + q_2^\rho q_2^\theta/m_2^2}{q_2^2 - m_2^2}\frac{-g^{\beta\tau} + q_3^\beta q_3^\tau/m_3^2}{q_3^2 - m_3^2}\prod_i \mathcal{F}_i(q_i^2). \tag{10}$$

Here p_1 (ε_1), p_2 (ε_2^*), and p_3 are the four-momenta (polarization vector) of the initial state $Z_b^{(\prime)}$, final state vector, and pseudoscalar mesons, respectively. q_1, q_2, and q_3 are the four-momenta of the up, right, and down bottomed mesons in the triangle loop, respectively.

Here we clarified whether the triangle singularity exists or not. The triangle singularity occurs when all the three internal particles can approach their on-shell condition simultaneously. In our cases, this condition requires the mass of the vector meson to be greater than or equal to the related $B\bar{B}^{(*)}$ threshold. Because the vector mesons are ρ and ω in the present work, this condition is impossible to satisfy. On the other hand, we also employ the criterion derived in Refs. [67,68] to check the statement. The criterion is

$\det[\frac{1}{2}(m_i^2+m_j^2-(q_i-q_j)^2)]=0$, where m and q are the mass and momentum of the internal particles, respectively. Using this relation, we can see that there is no triangle singularity in the triangle loops of Figs. 1 and 2.

In the present work, we adopt the product of monopole form factors for each intermediate meson, which is

$$\prod_i \mathcal{F}_i(q_i^2)=\mathcal{F}_1(q_1^2)\mathcal{F}_2(q_2^2)\mathcal{F}_3(q_3^2) \tag{11}$$

with

$$\mathcal{F}_i(q_i^2)=\frac{m^2-\Lambda^2}{q_i^2-\Lambda^2}. \tag{12}$$

The parameter Λ can be further reparametrized as $\Lambda_{B^{(*)}}=m_{B^{(*)}}+\alpha\Lambda_{\rm QCD}$ [65] with $\Lambda_{\rm QCD}=0.22$ GeV and $m_{B^{(*)}}$ is the mass of the intermediate bottomed meson. The dimensionless model parameter α is of order of unity [69–72] but its exact value cannot be obtained from the first principle. In practice, the value of α is usually determined by comparing the theoretical calculations with the corresponding experimental measurements. However, no light hadronic decay modes of $Z_b^{(\prime)}$ are known so far. For the rescattering processes studied in this work, it is found that monopole or dipole form factors for the exchanged particle are utilized, the numerical results are very sensitive to the values of α, and we have to use a very small value; otherwise, these partial decay widths will be very large, even more than the total width of $Z_b^{(\prime)}$. To avoid too large dependence of the parameter α, we take the form factor of Eq. (11) in the numerical calculations.

III. NUMERICAL RESULTS AND DISCUSSIONS

In this section, we present our numerical results for $Z_b^{(\prime)}\to VP$. The only model parameter in our model is the cutoff parameter α introduced in Eq. (11). No light hadron decay modes of Z_b and Z_b' are known so far. For the processes $Z_b^{(\prime)}\to VP$, we expect a relatively small value based on the following reasons. On the one hand, since the masses of Z_b and Z_b' are very close to the thresholds of $B\bar{B}^*$ and $B^*\bar{B}^*$, respectively, the threshold effects would be significantly enhanced. On the other hand, the phase space of the light hadron decay of $Z_b^{(\prime)}$ states is very large. We therefore take $\alpha=0.1$–0.3 to estimate the light hadron decays of $Z_b^{(\prime)}$.

In Figs. 3 and 4, we present the α dependence of the branching ratios of $Z_b\to VP$ and $Z_b'\to VP$ with the $\eta-\eta'$ mixing angle $\theta_P=-19.1°$, respectively. In the range of $\alpha=0.1$–0.3, the predicted branching ratios of $Z_b\to VP$ are about in the order of 10^{-2}, while for $Z_b'\to VP$ they are in the order of 10^{-3}. The predicted branching ratios of $Z_b\to VP$ are about 1 order of magnitude larger than those of $Z_b'\to VP$. As shown in Figs. 1 and 2, there are three

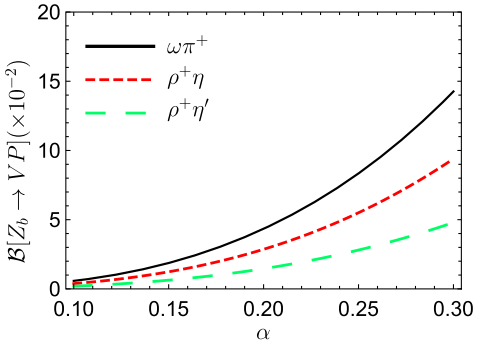

FIG. 3. The α dependence of the branching ratios of $Z_b\to VP$. Here the $\eta-\eta'$ mixing angle $\theta_P=-19.1°$ is taken from Refs. [73,74].

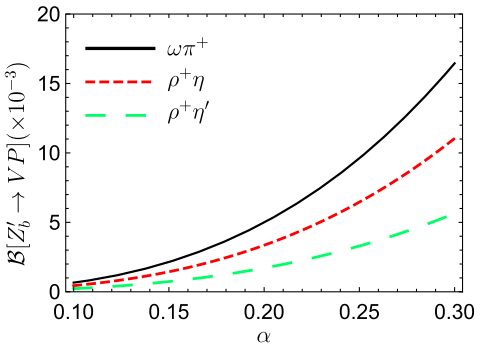

FIG. 4. The α dependence of the branching ratios of $Z_b'\to VP$. Here the $\eta-\eta'$ mixing angle $\theta_P=-19.1°$ is taken from Refs. [73,74].

kinds of diagrams for $Z_b\to VP$, while there are only two kinds for $Z_b'\to VP$. At the same α, the predicted branching ratios of $Z_b^{(\prime)}\to\rho^+\eta$ are larger than those of $Z_b^{(\prime)}\to\rho^+\eta'$, which is mainly due to the larger $n\bar{n}$ component in η. This point needs experimental confirmation in the future. From Eq. (7), we can obtain that $\theta_P=-19.1°$ corresponds to 66% $n\bar{n}$ component in η and 34% $n\bar{n}$ component in η'. In our calculations, we consider Z_b and Z_b' as $B\bar{B}^*+$c.c. and $B^*\bar{B}^*$ molecular states, respectively. We only calculate the contribution from neutral and charged bottomed meson loops; thus the larger branching ratio of $Z_b^{(\prime)}\to\rho^+\eta$ larger than that of $Z_b^{(\prime)}\to\rho^+\eta'$ is understandable. In the range of $\alpha=0.1$–0.3, the predicted branching ratios are about

$$\begin{aligned}
\mathcal{B}[Z_b\to\omega\pi^+]&=(0.58\text{–}14.3)\times10^{-2},\\
\mathcal{B}[Z_b\to\rho^+\eta]&=(0.38\text{–}9.40)\times10^{-2},\\
\mathcal{B}[Z_b\to\rho^+\eta']&=(0.20\text{–}4.80)\times10^{-2},\\
\mathcal{B}[Z_b'\to\omega\pi^+]&=(0.66\text{–}16.4)\times10^{-3},\\
\mathcal{B}[Z_b'\to\rho^+\eta]&=(0.44\text{–}11.0)\times10^{-3},\\
\mathcal{B}[Z_b'\to\rho^+\eta']&=(0.23\text{–}5.64)\times10^{-3}.
\end{aligned} \tag{13}$$

It would be interesting to further clarify the uncertainties arising from the introduction of the form factors by studying the α dependence of the ratios among different branching ratios. For the decays $Z_b \to VP$, we define the following ratios to the branching ratios of $Z_b \to \omega\pi^+$:

$$R_1 = \frac{\mathcal{B}[Z_b \to \rho^+\eta]}{\mathcal{B}[Z_b \to \omega\pi^+]},$$
$$R_2 = \frac{\mathcal{B}[Z_b \to \rho^+\eta']}{\mathcal{B}[Z_b \to \omega\pi^+]}. \quad (14)$$

Similarly, for the decays $Z_b' \to VP$ the ratios are defined as

$$r_1 = \frac{\mathcal{B}[Z_b' \to \rho^+\eta]}{\mathcal{B}[Z_b' \to \omega\pi^+]},$$
$$r_2 = \frac{\mathcal{B}[Z_b' \to \rho^+\eta']}{\mathcal{B}[Z_b' \to \omega\pi^+]}. \quad (15)$$

In Figs. 3 and 4, we use $\alpha = 0.1$–0.3 to estimate the branching ratios of $Z_b^{(\prime)} \to VP$. It is natural to use the same α range to estimate the ratios R_1 and R_2. The ratios R_i and r_i $(i = 1, 2)$ in terms of α are plotted in Fig. 5 with $\alpha = 0.1$–0.3. On the one hand, it shows that the ratios are almost independent of α, which indicates a reasonably controlled cutoff for each channel by the form factor to some extent. On the other hand, one can see that there is a certain dependence of the ratio on the $\eta - \eta'$ mixing angle θ_P, which is of more fundamental significance than the parameter α. This finding stimulates us to study the mixing angle θ_P dependence.

As is well known, the $\eta - \eta'$ mixing is a long-standing question in history. The mixing angle plays an important role in physical processes involving the η and η' mesons. However, the mixing angle can neither be calculated from first principles in QCD nor be directly measured from experiments. Next, we mainly focus on the impact of the mixing angle on the processes involving the η and η' mesons, namely $Z_b^{(\prime)} \to \rho^+\eta^{(\prime)}$. In Figs. 6 and 7, we plot the branching ratios of $Z_b \to \rho^+\eta^{(\prime)}$ and $Z_b' \to \rho^+\eta^{(\prime)}$ in terms

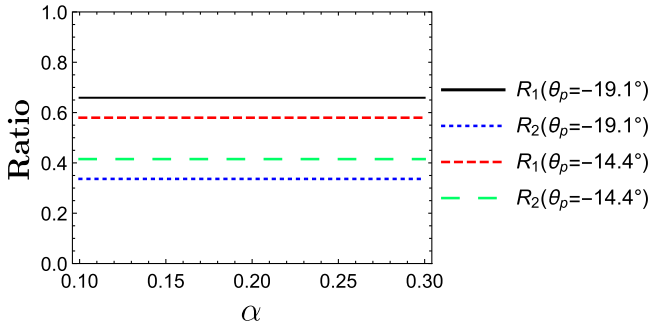

FIG. 5. The α dependence of the ratios R_1 and R_2 defined in Eq. (14) with $\theta_P = -19.1°$ [73,74] and $\theta_P = -14.4°$ [75].

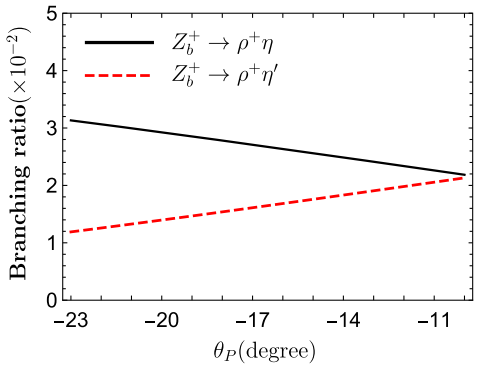

FIG. 6. Branching ratios of $Z_b \to \rho^+\eta^{(\prime)}$ depending on the mixing angle θ_P with $\alpha = 0.2$.

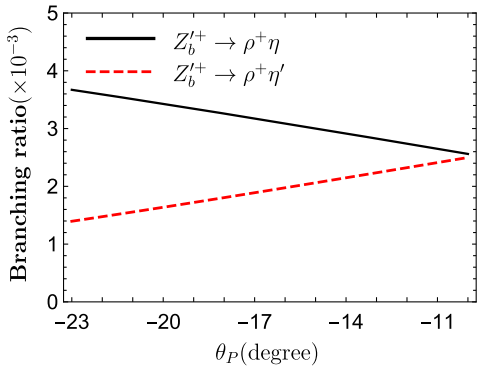

FIG. 7. Branching ratios of $Z_b' \to \rho^+\eta^{(\prime)}$ depending on the mixing angle θ_P with $\alpha = 0.2$.

of the $\eta - \eta'$ mixing angle with $\alpha = 0.2$. As shown in Fig. 6, when increasing the mixing angle θ_P, the branching ratio of $Z_b \to \rho^+\eta'$ increases, while the branching ratio of $Z_b \to \rho^+\eta$ decreases. This behavior suggests how the mixing angle influences our calculated results to some extent. As for $Z_b' \to \rho^+\eta^{(\prime)}$ in Fig. 7, the situation is similar.

In Fig. 8, we present the ratios defined in Eqs. (14) and (15) as a function of the mixing angle θ_P with $\alpha = 0.2$. It is interesting to see that the line shape behaviors of the ratios R_1 and r_1 are almost coincident and the same behaviors for the ratios R_2 and r_2. The $n\bar{n}$ components in η and η' and the intermediate bottomed meson loops may mainly influence these ratios. With the mixing angle range from $-23°$ to $-10°$, the ratios R_1 and r_1 decrease from 0.73 to 0.50, while the ratios R_2 and r_2 increase from 0.27 to 0.50. It is remarkable that these four ratios would be approximately equal at $\theta_P \simeq -10°$. We expect the future experiments could measure the ratios in Eqs. (14) and (15), which may help us constrain this mixing angle.

IV. SUMMARY

In this work, we evaluated the branching ratios of $Z_b^{(\prime)} \to VP$ by considering the contributions of intermediate bottomed meson triangle loops within an effective

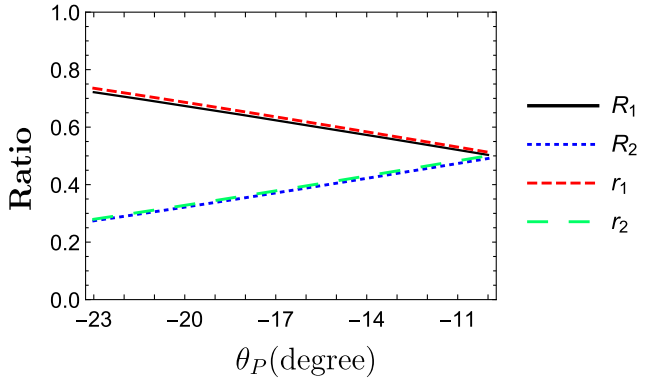

FIG. 8. Ratios defined in Eqs. (14) and (15) depending on θ_P with $\alpha = 0.2$.

Lagrangian approach, where the Z_b and Z_b' are assigned as $B\bar{B}^* + \text{c.c.}$ and $B^*\bar{B}^*$ molecular states, respectively. In the calculations, the quantum numbers of these two resonances are fixed to be $I^G(J^P) = 1^+(1^+)$, which is consistent with the experimental analysis. The predicted branching ratios of $Z_b \to VP$ are about in the order of 10^{-2}, while the branching ratios of $Z_b' \to VP$ are in the order of 10^{-3}. Moreover, the dependence of these ratios between different decay modes of $Z_b^{(\prime)}$ on the mixing $\eta - \eta'$ angle θ_P is also investigated, which may be a good quantity for the experiments. It is hoped that the calculations here can be tested by future experiments and can be used to determine the value of the mixing angle.

ACKNOWLEDGMENTS

Q. W. thanks Xiao-Hai Liu, Jun He, Qian Wang, and Ju-Jun Xie for useful discussions. This work is partly supported by the National Natural Science Foundation of China under Grants No. 12075133, No. 12105153, and No. 11835015, and the Natural Science Foundation of Shandong Province under Grant No. ZR2021MA082. It is also supported by Taishan Scholar Project of Shandong Province (Grant No. tsqn202103062), and the Higher Educational Youth Innovation Science and Technology Program Shandong Province (Grant No. 2020KJJ004).

[1] S. K. Choi *et al.* (Belle Collaboration), Phys. Rev. Lett. **91**, 262001 (2003).
[2] H.-X. Chen, W. Chen, X. Liu, and S.-L. Zhu, Phys. Rep. **639**, 1 (2016).
[3] A. Hosaka, T. Iijima, K. Miyabayashi, Y. Sakai, and S. Yasui, Prog. Theor. Exp. Phys. **2016**, 062C01 (2016).
[4] R. F. Lebed, R. E. Mitchell, and E. S. Swanson, Prog. Part. Nucl. Phys. **93**, 143 (2017).
[5] A. Esposito, A. Pilloni, and A. D. Polosa, Phys. Rep. **668**, 1 (2016).
[6] F.-K. Guo, C. Hanhart, U.-G. Meißner, Q. Wang, Q. Zhao, and B.-S. Zou, Rev. Mod. Phys. **90**, 015004 (2018).
[7] A. Ali, J. S. Lange, and S. Stone, Prog. Part. Nucl. Phys. **97**, 123 (2017).
[8] S. L. Olsen, T. Skwarnicki, and D. Zieminska, Rev. Mod. Phys. **90**, 015003 (2018).
[9] M. Karliner, J. L. Rosner, and T. Skwarnicki, Annu. Rev. Nucl. Part. Sci. **68**, 17 (2018).
[10] C.-Z. Yuan, Int. J. Mod. Phys. A **33**, 1830018 (2018).
[11] Y. Dong, A. Faessler, and V. E. Lyubovitskij, Prog. Part. Nucl. Phys. **94**, 282 (2017).
[12] Y. R. Liu, H. X. Chen, W. Chen, X. Liu, and S. L. Zhu, Prog. Part. Nucl. Phys. **107**, 237 (2019).
[13] H. X. Chen, W. Chen, X. Liu, Y. R. Liu, and S. L. Zhu, Rep. Prog. Phys. **86**, 026201 (2023).
[14] L. Meng, B. Wang, G. J. Wang, and S. L. Zhu, arXiv:2204.08716.
[15] M. Ablikim *et al.* (BESIII Collaboration), Phys. Rev. Lett. **110**, 252001 (2013).
[16] M. Ablikim *et al.* (BESIII Collaboration), Phys. Rev. Lett. **126**, 102001 (2021).
[17] R. Aaij *et al.* (LHCb Collaboration), Nat. Phys. **18**, 751 (2022).
[18] R. Aaij *et al.* (LHCb Collaboration), Nat. Commun. **13**, 3351 (2022).
[19] R. Aaij *et al.* (LHCb Collaboration), Sci. Bull. **65**, 1983 (2020).
[20] R. Aaij *et al.* (LHCb Collaboration), Phys. Rev. Lett. **115**, 072001 (2015).
[21] R. Aaij *et al.* (LHCb Collaboration), Phys. Rev. Lett. **122**, 222001 (2019).
[22] R. Aaij *et al.* (LHCb Collaboration), Phys. Rev. Lett. **128**, 062001 (2022).
[23] R. Aaij *et al.* (LHCb Collaboration), Sci. Bull. **66**, 1278 (2021).
[24] LHCb Collaboration, arXiv:2210.10346.
[25] A. Bondar *et al.* (Belle Collaboration), Phys. Rev. Lett. **108**, 122001 (2012).
[26] I. Adachi (Belle Collaboration), arXiv:1105.4583.
[27] A. Garmash *et al.* (Belle Collaboration), Phys. Rev. D **91**, 072003 (2015).
[28] I. Adachi *et al.* (Belle Collaboration), arXiv:1207.4345.
[29] P. Krokovny *et al.* (Belle Collaboration), Phys. Rev. D **88**, 052016 (2013).
[30] A. E. Bondar, A. Garmash, A. I. Milstein, R. Mizuk, and M. B. Voloshin, Phys. Rev. D **84**, 054010 (2011).
[31] Z.-F. Sun, J. He, X. Liu, Z.-G. Luo, and S.-L. Zhu, Phys. Rev. D **84**, 054002 (2011).
[32] T. Mehen and J. W. Powell, Phys. Rev. D **84**, 114013 (2011).
[33] M. Cleven, F.-K. Guo, C. Hanhart, and U.-G. Meißner, Eur. Phys. J. A **47**, 120 (2011).

[34] J. M. Dias, F. Aceti, and E. Oset, Phys. Rev. D **91**, 076001 (2015).
[35] M.-T. Li, W. L. Wang, Y.-B. Dong, and Z.-Y. Zhang, J. Phys. G **40**, 015003 (2013).
[36] Y. Yang, J. Ping, C. Deng, and H.-S. Zong, J. Phys. G **39**, 105001 (2012).
[37] J.-R. Zhang, M. Zhong, and M.-Q. Huang, Phys. Lett. B **704**, 312 (2011).
[38] Z.-G. Wang and T. Huang, Eur. Phys. J. C **74**, 2891 (2014).
[39] Z.-G. Wang, Eur. Phys. J. C **74**, 2963 (2014).
[40] Y. Dong, A. Faessler, T. Gutsche, and V. E. Lyubovitskij, J. Phys. G **40**, 015002 (2013).
[41] S. Ohkoda, S. Yasui, and A. Hosaka, Phys. Rev. D **89**, 074029 (2014).
[42] G. Li, F.-l. Shao, C.-W. Zhao, and Q. Zhao, Phys. Rev. D **87**, 034020 (2013).
[43] M. Cleven, Q. Wang, F.-K. Guo, C. Hanhart, U.-G. Meißner, and Q. Zhao, Phys. Rev. D **87**, 074006 (2013).
[44] X. Li and M. B. Voloshin, Phys. Rev. D **86**, 077502 (2012).
[45] G. Li, X.-H. Liu, and Z. Zhou, Phys. Rev. D **90**, 054006 (2014).
[46] C.-J. Xiao and D.-Y. Chen, Phys. Rev. D **96**, 014035 (2017).
[47] Q. Wu, D. Y. Chen, and T. Matsuki, Phys. Rev. D **102**, 114037 (2020).
[48] Q. Wu, D. Y. Chen, and F. K. Guo, Phys. Rev. D **99**, 034022 (2019).
[49] M. B. Voloshin, Phys. Rev. D **84**, 031502 (2011).
[50] T. Guo, L. Cao, M. Z. Zhou, and H. Chen, arXiv:1106.2284.
[51] C.-Y. Cui, Y.-L. Liu, and M.-Q. Huang, Phys. Rev. D **85**, 074014 (2012).
[52] Z.-G. Wang and T. Huang, Nucl. Phys. **A930**, 63 (2014).
[53] D. Y. Chen and X. Liu, Phys. Rev. D **84**, 094003 (2011).
[54] D. Y. Chen, X. Liu, and T. Matsuki, Chin. Phys. C **38**, 053102 (2014).
[55] D. V. Bugg, Europhys. Lett. **96**, 11002 (2011).
[56] E. S. Swanson, Phys. Rev. D **91**, 034009 (2015).
[57] I. Adachi *et al.* (Belle Collaboration), arXiv:1209.6450.
[58] R. L. Workman *et al.* (Particle Data Group), Prog. Theor. Exp. Phys. **2022**, 083C01 (2022).
[59] Q. Wu, G. Li, F. Shao, and R. Wang, Phys. Rev. D **94**, 014015 (2016).
[60] Y. Wang, Q. Wu, G. Li, W. H. Qin, X. H. Liu, C. S. An, and J. J. Xie, Phys. Rev. D **106**, 074015 (2022).
[61] F. K. Guo, C. Hanhart, Q. Wang, and Q. Zhao, Phys. Rev. D **91**, 051504 (2015).
[62] M. E. Peskin and D. V. Schroeder, *An Introduction to Quantum Field Theory* (Addison-Wesley, Reading, MA, 1995), p. 842.
[63] R. Casalbuoni, A. Deandrea, N. Di Bartolomeo, R. Gatto, F. Feruglio, and G. Nardulli, Phys. Rep. **281**, 145 (1997).
[64] P. Colangelo, F. De Fazio, and T. N. Pham, Phys. Rev. D **69**, 054023 (2004).
[65] H. Y. Cheng, C. K. Chua, and A. Soni, Phys. Rev. D **71**, 014030 (2005).
[66] C. Isola, M. Ladisa, G. Nardulli, and P. Santorelli, Phys. Rev. D **68**, 114001 (2003).
[67] F. K. Guo, X. H. Liu, and S. Sakai, Prog. Part. Nucl. Phys. **112**, 103757 (2020).
[68] X. H. Liu, M. Oka, and Q. Zhao, Phys. Lett. B **753**, 297 (2016).
[69] N. A. Tornqvist, Nuovo Cimento Soc. Ital. Fis. A **107**, 2471 (1994).
[70] N. A. Tornqvist, Z. Phys. C **61**, 525 (1994).
[71] M. P. Locher, Y. Lu, and B. S. Zou, Z. Phys. A **347**, 281 (1994).
[72] X. Q. Li, D. V. Bugg, and B. S. Zou, Phys. Rev. D **55**, 1421 (1997).
[73] D. Coffman *et al.* (MARK-III Collaboration), Phys. Rev. D **38**, 2695 (1988); **40**, 3788(E) (1989).
[74] J. Jousset *et al.* (DM2 Collaboration), Phys. Rev. D **41**, 1389 (1990).
[75] F. Ambrosino, A. Antonelli, M. Antonelli, F. Archilli, P. Beltrame, G. Bencivenni, S. Bertolucci, C. Bini, C. Bloise, S. Bocchetta *et al.*, J. High Energy Phys. 07 (2009) 105.